Mathematics in Applied Sciences and Engineering
Volume **3**, Number **2**, **2022**, pp.**106-118**
https://ojs.lib.uwo.ca/mase
https://doi.org/10.5206/mase/14625

MODELING ROAD SURFACE POTHOLES WITHIN THE MACROSCOPIC FLOW FRAMEWORK

GABRIEL O. FOSU, JOSEPH M. OPONG, BRIGHT E. OWUSU, AND SAMUEL M. NAANDAM

Abstract. The continual wearing of road surfaces results to crack and holes called potholes. These road surface irregularities often elongate travel time. In this paper, a second-order macroscopic traffic model is therefore proposed to account for these road surface irregularities that affect the smooth flow of vehicular traffic. Though potholes do vary in shape and size, for simplicity the paper assumes that all potholes have conic resemblances. The impact of different sized potholes on driving is experimented using fundamental diagrams. Besides, the width of these holes, driver reaction time amid these irregularities also determine the intensity of the flow rate and vehicular speed. Moreover, a local cluster analysis is performed to determine the effect of a small disturbance on flow. The results revealed that the magnitude of amplification on a road surface with larger cracks is not as severe as roads with smaller size holes, except at minimal and jam density where all amplifications quickly fade out.

1. Introduction

Traffic flow models have evolved from simple microscopic to complex macroscopic and mesoscopic models. Macroscopic models are either of first-order or second-order. The model by [22, 30] is known to be the inaugural offshoot of the first-order macroscopic branch. The second-order type was introduced by Payne[25], and Whitham[36], to fill the modeling gap of the first-order equation. The classical Payne's model was not invariant with respect to direction. Thus, in the early 2000s some second-order models were developed to address the backward wave traveling phenomena of Payne's model [4, 16, 29, 38]. Subsequently, extensive work has been done in relation to second-order macroscopic traffic models [9, 12, 19, 31]. All second-order macroscopic traffic models have followed Payne's conceptualization.

An aspect of traffic modeling is the impact of road surface conditions on vehicular flow. Some authors have developed a number of mathematical models to explain this connective conjecture [7, 32, 33]. In [7], the authors modeled the effect of best and worst road conditions on flow using explicit equations; one equation to model best road condition and the other to explain the worst road condition. In another paper[33] the authors developed a car-following model with consideration of varying road condition based on empirical data. An advantage of the model was the ability to qualitatively describe the effect of road condition on the micro driving behavior. A similar model was formulated using macroscopic properties [32], while [14] proposed a model to describe the effect of road, institutional and weather conditions on the traffic flow. This model used the data-driven approach.

Another observable road surface phenomena not yet accounted for within the macroscopic modeling domain is potholes. Potholes are significant feature of many parts of the highway network in third-world countries. Beside cause driving discomfort, its adverse effect is not limited to sudden deflation

Received by the editors 24 January 2022; accepted 5 May 2022; published online 15 May 2022.
2010 *Mathematics Subject Classification.* 35Q35, 76M20.
Key words and phrases. Higher-order traffic models, upwind finite difference, LWR model, bad roads, cluster effect, speed-density equation.

of pneumatic tires, speed fluctuations cause passenger jerking, and steering misalignment [21]. These potholes can be a nightmare for road-users. They are usually formed as a direct result of snow, ice, and prolonged periods of rain. Potholes frequently begin as undetectable microscopic cracks in the road surface. They are created when water penetrates these tiny cracks on the road-cracks that are usually caused by traffic. When this water penetrates, it expands and widens the cracks as traffic thumps down on these spaces. Extreme weather conditions, poor drainage, and heavy traffic can all cause that surface to loosen and wear away. Moreover, this deterioration causes unnecessary delays in traffic flow, distorts pavement aesthetics, and also causes road traffic accidents [23].

Even though potholes are observable road characteristic, the relation between potholes and macroscopic traffic characteristics is still a grey research area. It is imperative to know that literature on potholes is related to its detection [3, 6, 8, 15] but not to its modeling as is the intent of this research. Therefore, the paper seeks to derive a new second-order macroscopic model that accounts for these road surface irregularities. The classical second-order macroscopic model is extended to characterize pothole effect.

The subsequent sections are organized as follows. A new macroscopic traffic model is derived in section two to consider vehicular road potholes. In sections three, the model is subjected to realistic data values to examine the effect of these holes on the fundamental plot. Following-up with section four, we explore how a small disturbance propagates on the road with diverse irregularities. The final section presents a general summary of the entire work.

2. Second-Order Pothole Model

The two main branches of macroscopic traffic models are first-order and second-order classes of models. Second-order models are oftentimes referred to as higher-order models. Macroscopic models have a continuous property with respect to space and time as opposed to discrete models. Macroscopic models aggregate its quantities and possess continuous feature along both temporal and spatial axes. The three main aggregate variables required for macroscopic analysis are traffic density $k(x,t)$, average speed $u(x,t)$, and traffic flow rate $q(x,t)$. Two classical traffic equations relate these variables; the hydrodynamic equation, and the continuity or LWR equation [1, 11]. The hydrodynamic equation is expressed mathematically as:

$$q(x,t) = k(x,t) \cdot u(x,t) \tag{2.1}$$

The second relation, called the LWR, is also expressed as:

$$k_t + q_x = 0 \rightarrow k_t + (ku)_x = 0 \tag{2.2}$$

In reducing the boredom of continual writing the bracketed spatial and temporal notations (x,t), it is often omitted as in the case of Equation (2.2), and will follow suit in all other subsequent formulations.

The continuity equation is famous because of its simplicity and realistic efficiency. Compared to other macroscopic models, the LWR is known to be simplest based on the parsimony principle. However, the LWR model is handicapped for its inability to explain non-equilibrium traffic. This shortfall leads to the development of higher-order models. Higher-order models supplement the continuity equation with a dynamic velocity equation. A classical speed-gradient second-order model is of the form[16]:

$$k_t + (ku)_x = 0 \tag{2.3}$$

$$u_t + uu_x = \frac{U(k_e) - u}{\tau} + c_o u_x \tag{2.4}$$

$U(k_e)$ is the steady state speed, τ is the relaxation time, and c_o is the propagation speed of a small disturbance.

As emphasized in the introduction, an additional source term is to be added to the dynamic velocity equation to characterize the effect of potholes on vehicular traffic. From [13, 26, 27], a road surface irregularity $r(\theta)$ can be generated using equation (2.5).

$$r(\theta) = \begin{cases} -\frac{\alpha}{2}\left(1 - \cos\frac{2\pi\theta}{\beta}\right), & 0 \le \theta \le \beta \\ 0, & \theta < 0, \theta > b \end{cases} \tag{2.5}$$

where α is the depth of the pothole; $\alpha < 0$ corresponds to bulge road surface. $\beta > 0$ is the width of the pothole, θ is any location within the pothole measured starting from the leftmost endpoint. Unique depth and width values will result in unique pothole sizes. Figures 1 and 2 show different sizes of potholes differing by width and depth.

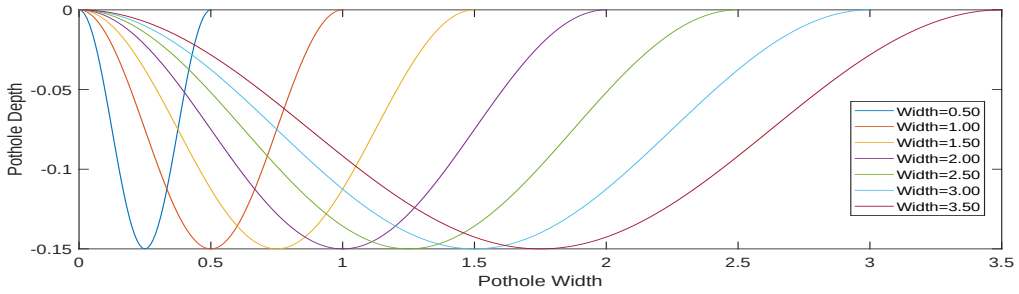

FIGURE 1. Different Pothole Sizes with Variable Depth

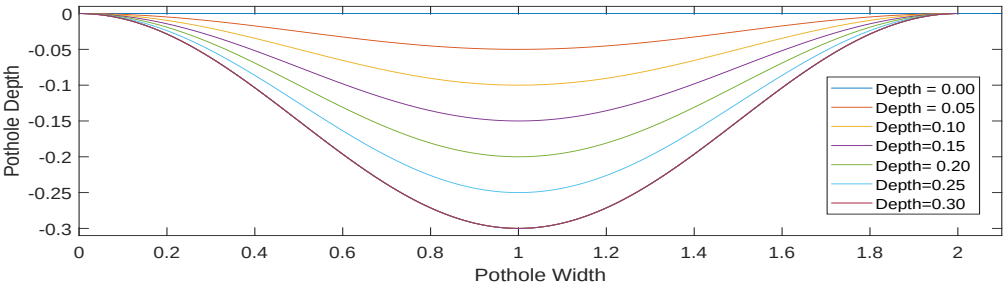

FIGURE 2. Different Pothole Sizes with Variable Depth

Figure 1 shows seven different potholes with a width ranging from 0.5 meters to 3.5 meters, having a constant depth of 0.15 meters. Potholes with absurd widths ($\beta > 1.5$) are characteristic of feeder roads. In Figure 2 are potholes having fixed width of two meters and a depth ranging from zero to 0.30 meters. Zero depth denotes a normal/smooth road surface devoid of any form of cracks or holes.

It could be observed that Figures 1 and 2 have close similitude to a hollow cone. This assumption is associated with some margin of error considering each hole as a microscopic entity. Nonetheless, the errors may wane or extinct within the macroscopic framework due to variable aggregation. Therefore, to quantize these road surface irregularity, all potholes are assumed to be cone-like, though with a shorter vertical height. On this premise, a given pothole size (S_p) can be approximated using equation (2.6).

$$S_p = -\frac{1}{2}\pi\beta\sqrt{\frac{\beta^2}{4} + \alpha^2} \tag{2.6}$$

As stated earlier, road surface irregularity is known to have some impact on vehicular flow, but the intensity of this impact depends much on the density of the traffic as well. For highly dense traffic, the effect of potholes is not so substantial compared to fairly moving traffic. The speed changes resulting from some road surface irregularity on a near empty road vast exceed that of dense traffic. This to say that the overall effect of these irregularities on flow during jam traffic may be insignificant. This analogy is incorporated in the derivation, yielding the modified form of (2.6) as:

$$T_p = \begin{cases} -\frac{1}{2}\pi\beta T\sqrt{\left(\frac{\beta^2}{4}+\alpha^2\right)}\left(1-\frac{k}{k_{crit}}\right), & k \le k_{crit} \\ 0, & \text{otherwise} \end{cases} \tag{2.7}$$

k_{crit} denote the critical density, and T is the driver physiological reaction time. The latter accounts for the varying response time among different type of drivers/vehicles. Aggressive drivers have little respect for potholes and will often maintain their speed driving through such irregularities, hence they are associated with shorter reaction time. Directly opposite to this group of drivers are the sluggish type who will slow down irrespective of the hole size. Moreover, vehicles with weaker shock absorbers often slow down driving through potholes. These classes of drivers/vehicles are associated with a greater T value.

Equation (2.7) is appended to the dynamic velocity equation to yield the new second-order macroscopic pothole traffic model. The proposed equation is expressed as

$$k_t + (ku)_x = 0 \tag{2.8}$$

$$u_t + uu_x = \frac{U(k_e)-u}{\tau} + c_o u_x - \frac{1}{2}\pi\beta T\sqrt{\left(\frac{\beta^2}{4}+\alpha^2\right)}\left(1-\frac{k}{k_{crit}}\right) \tag{2.9}$$

Equation (2.8) is the usual continuity equation, while (2.9) is the modified dynamic speed equation.

In the next section, the second-order pothole model is subjected to assumed realistic data values to examine the effect of different sized potholes on vehicular traffic.

3. Fundamental Diagrams

Fundamental plots are graphical representation of the pairwise relationship between speed, density, and flow. Some graphical illustrations are presented in this section to exemplify the effect of potholes on these macroscopic variables. For uniform flow, traffic characteristics, specifically density and speed, are invariant with respect to space and time. Hence, equation (2.9) reduce to:

$$\frac{U(k_e)-u_u}{\tau} - \frac{1}{2}\pi\beta T\sqrt{\left(\frac{\beta^2}{4}+\alpha^2\right)}\left(1-\frac{k_u}{k_{crit}}\right) = 0 \tag{3.1}$$

Uniform speed is denoted by u_u, while k_u represents uniform density. This equation (3.1) is again simplified as:

$$u_u = U(k_e) - \frac{1}{2}\pi\beta T\tau\sqrt{\left(\frac{\beta^2}{4}+\alpha^2\right)}\left(1-\frac{k_u}{k_{crit}}\right) \tag{3.2}$$

An equation for steady-state speed $U(k_e)$ is required for this qualitative analysis. Several of these equations have been presented in [10]. An appropriate choice among these speed-density models for this analysis is the exponential KK model (3.3) [17].

$$U(k_e) = u_{max}\left[1/\left\{1+\exp\left(\frac{\frac{k}{k_{max}}-0.25}{0.06}\right)\right\} - 372\times 10^{-8}\right] \tag{3.3}$$

where u_{max} denote the maximum attainable speed on a freeway, and k_{max} is the maximum density at jam traffic.

The assumed parameter values presented in Table 1 are used for the computations. These are chosen to be coherent with realistic traffic flow [18, 34].

TABLE 1. Simulation Parameters

Name	Notation	Value
Maximum Speed	u_{max}	$25m/s$
Relaxation time	τ	$1s$
Critical density	k_{crit}	$0.38veh/m$
Jam density	k_{max}	$1.0veh/m$
Reaction time	T	$[0.5\ 6]s$

These values are adopted to exemplify the pairwise relationship between speed-density and flow-density, taken into account different pothole widths and reaction times. In relation to sizes, potholes are categorized under three broad domains; namely small, medium, and large potholes. Potholes with a width of less than 0.5 meters is classified as small pothole. The width of large pothole category exceed 1.4 meters. Sandwich between the smaller and larger categories are the medium type of potholes. Similarly, drivers are also grouped into three based on their reaction time. It is assumed that aggressive drivers have a reaction time of 0.5 seconds, while the reaction time for sluggish drivers is 6 seconds. Any time seconds within the neighborhood of the mean times of aggressive and sluggish drivers correspond to normal driving.

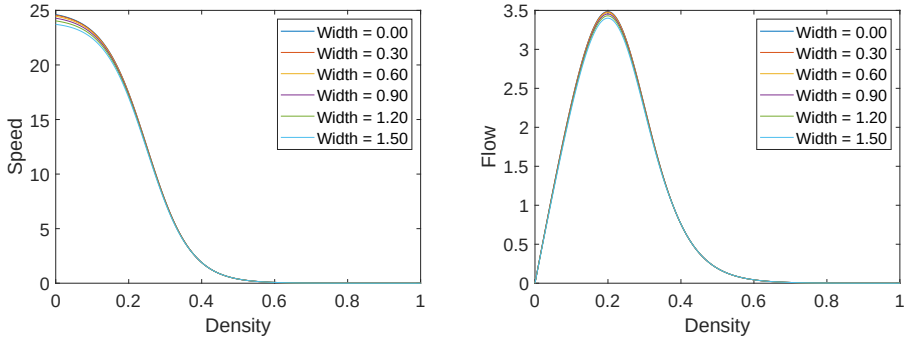

FIGURE 3. Impact of a pothole on speed-density plot (left), and flow-density plot (right) with $T = 0.5s$

Figure 3 exemplifies the fundamental plot of an aggressive driver for varying pothole sizes. These potholes have a constant depth of 0.15 meters, with varying width from zero to 1.5 meters. Starting the simulation from regular road surface (width=0.00), all subsequent simulations have width increment of 0.3 meters. Though not apparent, it can be observed that at lower densities, each simulation plot has its corresponding speed value, and then merges after the critical point.

For a near empty highway, aggressive drivers decrease their speed slightly below the maximum when driving through these potholes. The speed drop is totally insignificant for driving through holes with a width of 0.3 meters. We only see aggressive drivers slowing down driving through larger potholes. Likewise, from the flow-density plot, the effect of aggressive driving on flow rate is again not so remarkable. Flow rate is seen to drop from $3.5veh/s$ to $3.3999veh/s$ as the width is widened from zero to 1.5

meters. The flow rate on roads with these simulated surface irregularities is practically the same if all drivers drive aggressively.

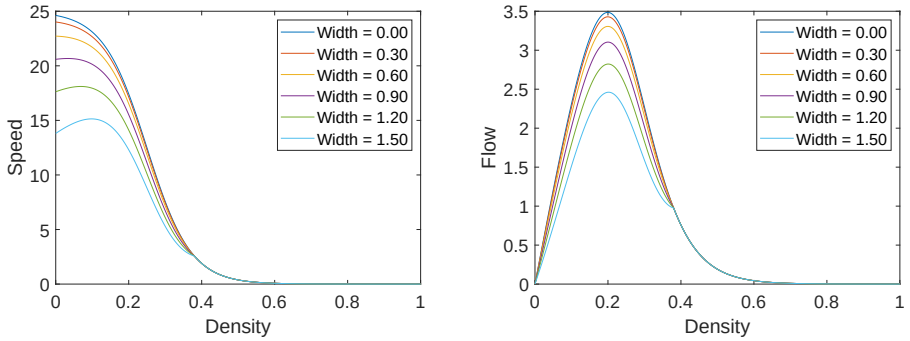

FIGURE 4. Impact of a pothole on speed-density plot (left), and flow-density plot (right) with $T = 6s$

Figure 4 is related to the case of sluggish driving. The speed drop is clearly evidential in this case. Bigger portholes cause sluggish drivers to reduce their speed to the neighborhood $15m/s$, but, maintains a speed limit between $[20m/s,\ 25m/s]$ driving through small and medium potholes. From an empty road to the critical density, the sizes of these road surface irregularities have a significant effect on vehicular speed within the domain of sluggish driving. However, the speed remains the same during jam traffic. This exhibit a practical exemplification of driving on the road with these irregularities. Similarly, the flow rate is also influenced by these irregularities. From Figure 4, flow is observed to increase, attain maximum value, and then decline. Flow rate is totally dependent on the width of these potholes.

A clear case for regular driving is shown in Figure 5 with an average reaction time of three seconds. This class of drivers are neither not too fast as aggressive nor too slow as sluggish. Except for width equal 1.5 meters, they could still attain a speed value greater than $20m/s$ driving through the simulated potholes. This has a corresponding effect on the flow-density diagram.

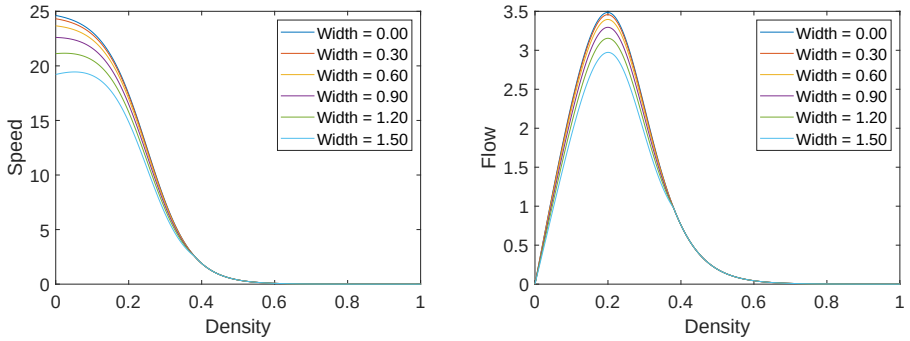

FIGURE 5. Impact of a pothole on speed-density plot (left), and flow-density plot (right) with $T = 3s$

Figure 6 shows the fundamental diagrams for road having potholes depths 0.05 meters (left) and 0.3 meters (right). Driver reaction time is assumed to be three seconds. It can be observed that the depth

of potholes on vehicular speed is not as substantial as the width exemplification. From the simulation, it can be actualized that the width of potholes highly induces vehicular speed/flow compared to its depth.

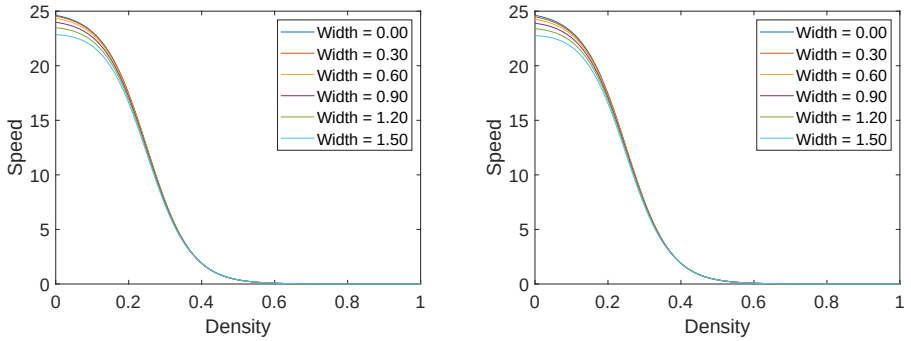

FIGURE 6. Impact of a pothole on speed-density plot with depth equal 0.05 (left), and depth equal 0.25 (right)

These road surface irregularities are characteristic of many roads in Ghana, an hour journey could span a minimum of two hours owing to these road surface irregularities [24, 28, 35], hence the essence of this model. This corroborates that improving road infrastructure will enhance the efficiency of vehicular flow.

4. Cluster Effect

The section investigates how a disturbance evolves on roads with differing surface irregularities. We inquire how a local perturbation propagates through space and time amidst such irregularities. Following from [16, 32] the finite difference upwind scheme is used to discretize the continuity equation (2.8) and the modified dynamic velocity equation (2.9). First, the continuity equation is simplified as $k_t + uk_x + ku_x = 0$ to ease the discretization. Hence, the discrete pothole model is given as:

$$k_m^{n+1} = k_m^n + \frac{\Delta t}{\Delta x} k_m^n \left(u_m^n - u_{m+1}^n\right) + \frac{\Delta t}{\Delta x} u_m^n \left(k_{m-1}^n - k_m^n\right) \tag{4.1}$$

The dynamic speed equation has two discrete cases. If the wave disturbance speed is higher than the vehicular speed, then the model is expressed as

$$u_m^{n+1} = u_m^n + \frac{\Delta t}{\Delta x}\left(c_o - u_m^n\right)\left(u_{m+1}^n - u_m^n\right) + \frac{\Delta t}{\tau}\left(U(k_m^n) - u_m^n\right) - \frac{\Delta t}{2}\pi\beta T\sqrt{\left(\frac{\beta^2}{4} + \alpha^2\right)}\left(1 - \frac{k_m^n}{k_{crit}}\right) \tag{4.2}$$

otherwise

$$u_m^{n+1} = u_m^n + \frac{\Delta t}{\Delta x}\left(c_o - u_m^n\right)\left(u_m^n - u_{m-1}^n\right) + \frac{\Delta t}{\tau}\left(U(k_m^n) - u_m^n\right) - \frac{\Delta t}{2}\pi\beta T\sqrt{\left(\frac{\beta^2}{4} + \alpha^2\right)}\left(1 - \frac{k_m^n}{k_{crit}}\right) \tag{4.3}$$

where $U(k_m^n)$ has the form

$$U(k_m^n) = u_{max}\left[1/\left\{1 + \exp\left(\frac{\frac{k_m^n}{k_{max}} - 0.25}{0.06}\right)\right\} - 372 \times 10^{-8}\right] \tag{4.4}$$

The simulation is subjected to a periodic boundary condition of the form

$$k(L,t) = k(0,t) \qquad \text{and} \qquad u(L,t) = u(0,t)$$

where L is the total length of roadway.

The initial density is given by the wave profile (4.5) [17].

$$k(x,0) = k_o + \Delta k_o \left\{ \cosh^{-2}\left[\frac{160}{L}\left(x - \frac{5L}{16}\right)\right] - \frac{1}{4}\cosh^{-2}\left[\frac{40}{L}\left(x - \frac{11L}{32}\right)\right]\right\} \tag{4.5}$$

with $v(x,0) = f(k(x,0))$. k_o is initial constant density, and Δk_o is the amplitude of the displacement.

The additional parameter values required for these wave amplification are detailed as follows. Δk_o is chosen as $0.20veh/m$, while k_o will range between $[0.10veh/m,\ 0.42veh/m]$. A road length $L = 1km$ is equally divided into 100 grid points. The simulation time is 10 minutes with the time step of 0.1 seconds. The wave disturbance speed $c_o = 9m/s$, the relaxation time $\tau = 3s$, and the reaction time $T = 1s$. k_{max}, k_{crit}, and u_{max} remain the same as in Table 1. Potholes will have the following specific dimensions as in Table 2.

TABLE 2. Pothole Groupings

Pothole Type	Width	Depth
Small	0.4m	0.1m
Medium	1.4m	0.2m
Large	2.4m	0.3m

The following commentaries are based on the graphical presentations 7-9. The amplifications on the road with smaller potholes is presented with Figure 7. These amplifications quickly dies-off when the initial density is within the neighborhood of its endpoints. This is clearly evinced when $k_o = 0.10$ and $k_o = 0.42$. These amplifications increase with an increasing number of vehicles on the stretch and then begin to flatten after reaching a critical density value. There are pieces of evidences of dipole and multiple clusters within $0.24veh/m$ and $0.28veh/m$. These are associated with stop-and-go traffic.

A similar effect could be realized considering the medium size and larger size potholes. These illustrations are presented in Figures 8 and 9, respectively. Again, the disruption dissolve quickly at the two extreme density values; $k_o = 0.10$ and $k_o = 0.42$. This implies that the effect of this disturbance does not propagate through space and time for near-empty traffic or close to jam density traffic. For medium densities, the amplification for large potholed road is not as severe as smaller once. The severity of road surface irregularities may cause drivers to slow down first [2, 5, 20, 37], hence reducing the net effect of any disturbance. Comparatively, the amplification for large sized potholed roads is quite stable.

In summary, this new second-order macroscopic pothole traffic model is useful for examining the dynamics of vehicular flow on roads with cracks and holes.

5. CONCLUSION

This study applies mathematical models to describe road surface potholes within the macroscopic flow framework. Potholes are created by the continual wearing of road surfaces resulting in cracks and holes. These irregularities have not been explicitly modeled within the ambit of macroscopic models. Therefore, we proposed a second-order macroscopic equation to explore the effect of these irregularities of vehicular traffic. To ease the computations, ro ad surface irregularities were categorized into three broad domains (small, medium, and large), and also assumed to be conical. A qualitative solution to the model was presented to illustrate the effect of these irregularities on the speed-density and flow-density plots. From the fundamental diagrams, speed was observed to reduce drastically, driving through these

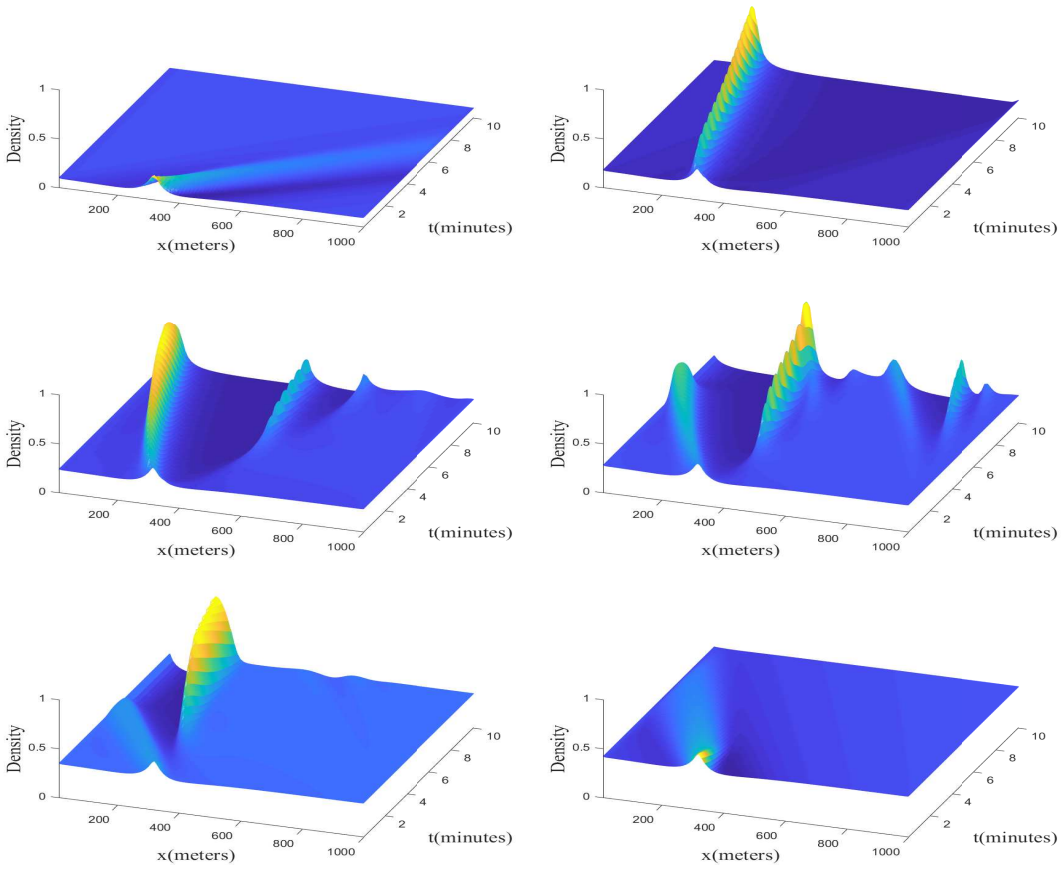

FIGURE 7. Space-time evolution of density on small size pothole road. The initial density profiles are given as $k_o = 0.10$(top left), $k_o = 0.18$(top right), $k_o = 0.24$(middle left), $k_o = 0.28$(middle right), $k_o = 0.35$(bottom left), $k_o = 0.42$(bottom right)

potholes as in the case of sluggish driving. The differences in the flow rate were not evident, as in the case of a platoon of aggressive drivers. However, all vehicles-driver type were observed to possess the same speed and flow characteristics beyond a critical density value. Showing a clear conceptualization of realistic flow. A further simulation was carried out to determine the effect of a small perturbation on uniform traffic. What is often referred to as the local cluster effect. The amplifications were observed to be negativity related to pothole sizes but within specific density values. The degree of the disturbance increases as the holes become smaller. However, the disruption quickly dies-off when there are either few vehicles on the stretch or close to jam density traffic. These simulations suggest that the proposed model is potent in exploring diverse traffic phenomena on roads with potholes. The possible extension is to analyze road surface irregularity microscopically.

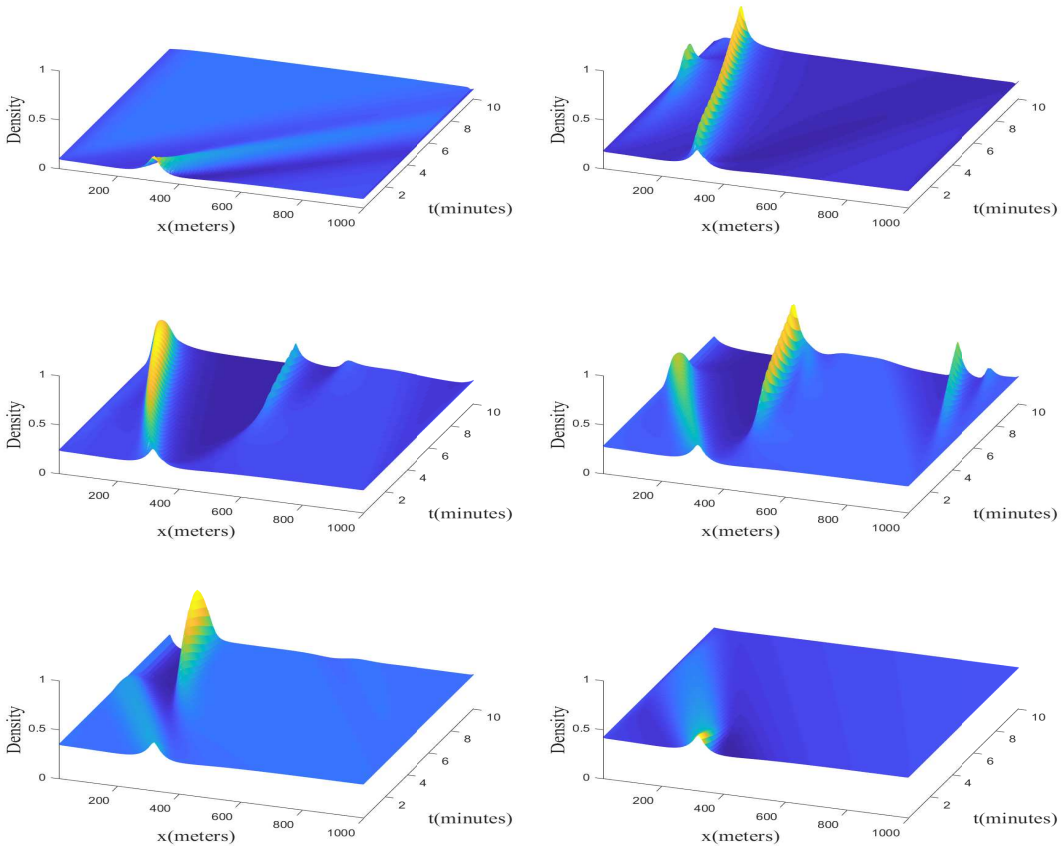

FIGURE 8. Space-time evolution of density on medium size pothole road. The initial density profiles are given as $k_o = 0.10$(top left), $k_o = 0.18$(top right), $k_o = 0.24$(middle left), $k_o = 0.28$(middle right), $k_o = 0.35$(bottom left), $k_o = 0.42$(bottom right)

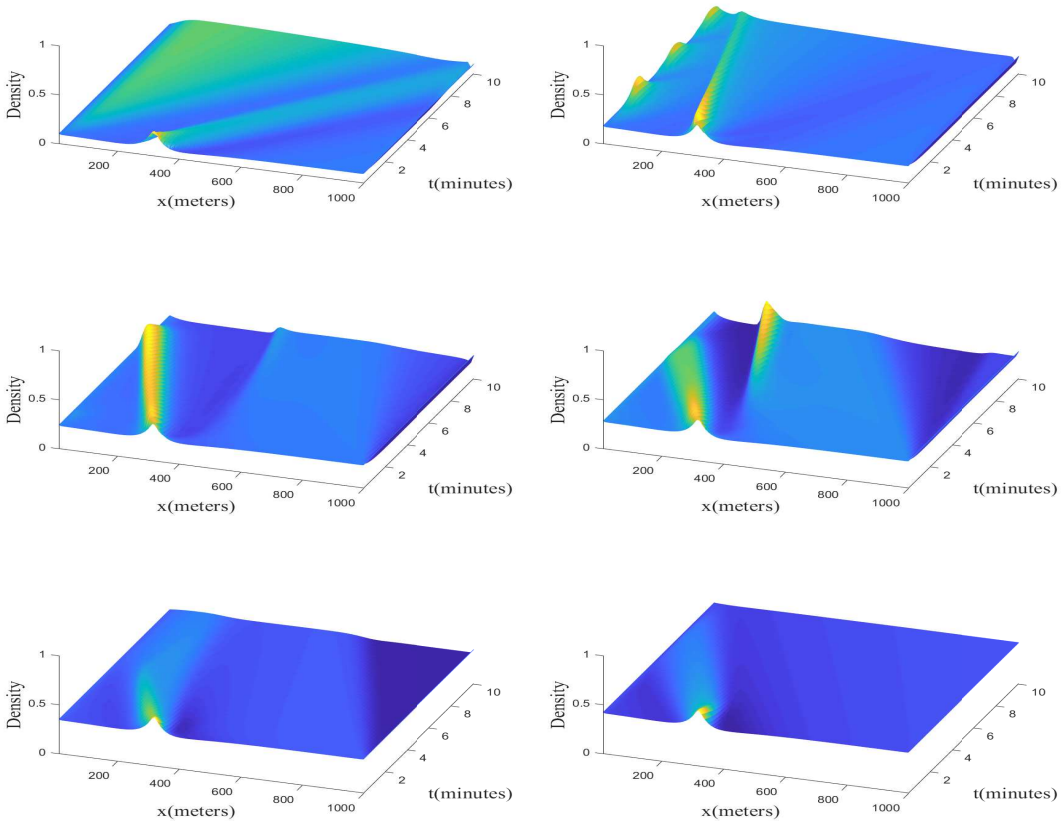

FIGURE 9. Space-time evolution of density on large size pothole road. The initial density profiles are given as $k_o = 0.10$(top left), $k_o = 0.18$(top right), $k_o = 0.24$(middle left), $k_o = 0.28$(middle right), $k_o = 0.35$(bottom left), $k_o = 0.42$(bottom right)

References

[1] E. Akweittey and G. O. Fosu, *A critical analysis of multi-regime fundamental equations*, J. Eng Res. Reports **6** (2019), 1–8.

[2] M. Y. Alam, A. Nandi, A. Kumar, S. Saha, M. Saha, S. Nandi, and S. Chakraborty, *Crowdsourcing from the true crowd: Device, vehicle, road-surface and driving independent road profiling from smartphone sensors*, Pervasive Mob. Comput. **61** (2020), 101103.

[3] S. Arjapure and D. R. Kalbande, *Review on analysis techniques for road pothole detection*, Soft Computing: Theories and Applications, Springer, 2020, 1189–1197.

[4] A. Aw and M. Rascle, *Resurrection of "second order" models of traffic flow*, SIAM J. Appl. Math. **60** (2000), 916–938.

[5] P. P. Awari and A. Menon, *Study on repairing of potholes*, VIVA-Tech International Journal for Research and Innovation **1** (2021), 1–6.

[6] K. Bansal, K. Mittal, G. Ahuja, A. Singh, and S. S. Gill, *Deepbus: Machine learning based real time pothole detection system for smart transportation using IOT*, Internet Technol. Lett. **3** (2020), 156.

[7] A. Bellouquid and M. Delitala, *Asymptotic limits of a discrete kinetic theory model of vehicular traffic*, Appl. Math. Lett. **24** (2011), 672–678.

[8] J. Dharneeshkar, S.A. Aniruthan, R. Karthika, L. Parameswaran, *Deep learning based detection of potholes in Indian roads using Yolo*, 2020 International Conference on Inventive Computation Technologies (ICICT), IEEE, 2020, 381–385.

[9] G. Dimarco and A. Tosin, *The aw–rascle traffic model: Enskog-type kinetic derivation and generalisations*, J. Stat. Phys. **178** (2020), 178–210.

[10] G. O. Fosu, E. Akweittey, J. M. Opong, and M. E. Otoo, *Vehicular traffic models for speed-density-flow relationship*, J. Math. Model. **8** (2020), 241–255.

[11] G. O. Fosu and F. T. Oduro, *On the characteristic curves for single-regime traffic models*, J. Glob. Res. Math. Arch. **4** (2017), 1–8.

[12] G. O. Fosu and F. T. Oduro, *Two dimensional anisotropic macroscopic second-order traffic flow model*, J. Appl. Comput. Mech. **19** (2020), 59–71.

[13] L. Fryba, *Vibration of solids and structures under moving loads*, Thomas Telford Ltd., London, 1999.

[14] O. K. Golovnin, *Data-driven profiling of traffic flow with varying road conditions*, CEUR Workshop Proceedings, **2416**, 2019, 149–157.

[15] S. Gupta, P. Sharma, D. Sharma, V. Gupta, and N. Sambyal, *Detection and localization of potholes in thermal images using deep neural networks*, Multimed. Tools Appl. (2020), 1–20.

[16] R. Jiang, Q. S. Wu, and Z. J. Zhu, *A new continuum model for traffic flow and numerical tests*, Transp. Res. B: Methodol. **36** (2002), 405–419.

[17] B. S. Kerner and P. Konhäuser, *Structure and parameters of clusters in traffic flow*, Phys. Rev. E **50** (1994), 54–83.

[18] H. Z. Khan, W. Imran, S. Azeem, K. S. Khattak, T. A. Gulliver, and M. S. Aslam, *A macroscopic traffic model based on driver reaction and traffic stimuli*, Appl. Sci. **9** (2019), 2848.

[19] Z. H. Khan and T. A. Gulliver, *A macroscopic traffic model based on transition velocities*, J. Comput. Sci. (2020), 101131.

[20] M. Kotha, M. Chadalavada, S. H. Karuturi, and H. Venkataraman, *Potsense: Pothole detection on indian roads using smartphone sensors*, In Proceedings of the 1st ACM Workshop on Autonomous and Intelligent mobile systems (AIMS'20), 2020.

[21] Z. Li, I. Kolmanovsky, E. Atkins, J. Lu, and D. Filev, *Road anomaly estimation: Model based pothole detection*, 2015 American Control Conference (ACC), IEEE, 2015, 1315–1320.
[22] M. J. Lighthill and G. B. Whitham, *On kinematic waves II: A theory of traffic flow on long crowded roads*, Proc. R. Soc. Lond. **229** (1955), 317–345.
[23] O. M. Ogundipe, *Road pavement failure caused by poor soil properties along aramoko-ilesa highway, Nigeria*, J. Eng. Appl. Sci. **3** (2008), 239–241.
[24] K. Olagunju, *Evaluating traffic congestion in developing countries. a case study of Nigeria*, Journal of the Chartered Institute of Logistics and Transport-Nigeria **2** (2015), 23–26.
[25] H. J. Payne, *Models of freeway traffic and control*, In: G. A. Bekey (ed.) Mathematical Models of Public Systems (Simulation Council, La Jolla, CA) **1** (1971), 51–61.
[26] A. V. Pesterev, L. A. Bergman, and C. A. Tan, *A novel approach to the calculation of pothole-induced contact forces in MDOF vehicle models*, J. Sound Vib. **275** (2004), 127–149.
[27] A. V. Pesterev, L. A. Bergman, C. A. Tan, and B. Yang, *Assessing tire forces due to roadway unevenness by the pothole dynamic amplification factor method*, J. Sound Vib. **279** (2005), 817–841.
[28] M. Poku-Boansi, E. Ekekpe, A. A. Bonney, *Combating maternal mortality in the Gushegu district of Ghana: The role of rural transportation*, J. Sustainable Dev. Afr. **12** (2010), 274–283.
[29] M. Rascle, *An improved macroscopic model of traffic flow: derivation and links with the Lighthill Whitham model*, Math. Comput. Model. **35** (2002), 581–590.
[30] P. I. Richards, *Shock waves on the highway*, Oper. Res. **4** (1956), 42–51.
[31] M. H. Sadeghian, M. Gachpazan, N. Davoodi, and F. Toutounian, *A macroscopic second order model for air traffic flow*, J. Math. Model. **8** (2020), 41–54.
[32] T. Tang, L. Caccetta, Y. Wu, H. Huang, and X. Yang, *A macro model for traffic flow on road networks with varying road conditions*, J. Adv. Transp. **48** (2014), 304–317.
[33] T. Tang, Y. Wang, X. Yang, and Y. Wu, *A new car-following model accounting for varying road condition*, Nonlinear Dyn. **70** (2012), 1397–1405.
[34] M. Treiber and A. Kesting, *Traffic flow dynamics; data, models and simulation*, Springer-Verlag Berlin Heidelberg, 2013.
[35] D. K. Twerefou, P. Chinowsky, K. Adjei-Mantey, and N. L. Strzepek, *The economic impact of climate change on road infrastructure in Ghana*, Sustainability **7** (2015), 11949–11966.
[36] G. B. Whitham, *Linear and nonlinear waves*, John Wiley and Sons, New York, 1974.
[37] J. Yu, H. Zhu, H. Han, Y. J. Chen, J. Yang, Y. Zhu, Z. Chen, G. Xue, and M. Li, *Senspeed: Sensing driving conditions to estimate vehicle speed in urban environments*, IEEE Trans. Mob. Comput. **15** (2015), 202–216.
[38] H. M. Zhang, *A non-equilibrium traffic model devoid of gas-like behavior*, Transp. Res. B: Methodol. **36** (2002), 275–290.

Corresponding author, Department of Mathematics, Kwame Nkrumah University of Science and Technology, Kumasi, Ghana
Email address: gabriel.of@knust.edu.gh

Department of Mathematics, Presbyterian University College, Abetifi, Ghana
Email address: joeopong@presbyuniversity.edu.gh

Department of Mathematics, Kwame Nkrumah University of Science and Technology, Kumasi, Ghana
Email address: bright.owusu@knust.edu.gh

Department of Mathematics, University of Cape Coast, Cape Coast, Ghana
Email address: snaandam@ucc.edu.gh